[1] C. Niehrs, R. Beisswanger, W. B. Huttner, *Chem.-Biol. Interact.* **1994**, *92*, 257 – 271.
[2] a) M. Farzan, T. Mirzabekov, P. Kolchinsky, R. Wyatt, M. Cayabyab, N. P. Gerard, C. Gerard, J. Sodroski, H. Choe, *Cell* **1999**, *96*, 667 – 676; b) A. Leppanen, S. P. White, J. Helin, R. P. McEver, R. D. Cummings, *J. Biol. Chem.* **2000**, *275*, 39569 – 39578; c) E. G. Cormier, D. N. H. Tran, L. Yukhayeva, W. C. Olson, T. Dragic, *J. Virol.* **2001**, *75*, 5541 – 5549; c) J. Dong, P. Ye, A. J. Schade, S. Gao, G. M. Romo, N. T. Turner, L. V. McIntire, J. A. Lopez, *J. Biol. Chem.* **2001**, *276*, 16690; e) S. Costagliola, V. Panneels, M. Bonomi, J. Koch, M. C. Many, G. Smits, G. Vassart, *EMBO J.* **2002**, *21*, 504.
[3] W. S. Somers, J. Tan, G. D. Shaw, R. T. Camphausen, *Cell* **2000**, *103*, 467 – 479. For a review, see: J. W. Kehoe, C. R. Bertozzi, *Chem. Biol.* **2000**, *7*, R57-R61.
[4] a) Y. Kurano, T. Kimura, S. Sakakibara, *J. Chem. Soc. Chem. Commun.* **1987**, 323 – 325; b) N. Fujii, S. Futaki, S. Funakoshi, K. Akaji, H. Morimoto, R. Doi, K. Inoue, M. Kogire, S. Sumi, M. Yun, T. Tobe, M. Aono, M. Matsuda, H. Narusawa, M. Moriga, H. Yajima, *Chem. Pharm. Bull.* **1988**, *36*, 3281 – 3291; c) K. Kitagawa, S. Futaki, T. Yagami, *J. Synth. Org. Chem. Jpn.* **1994**, *52*, 675 – 685.
[5] a) K. Barlos, D. Gatos, J. Kallitsis, G. Papaphotiu, P. Sotiriu, W. Q. Yao, W. Schafer, *Tetrahedron Lett.* **1989**, *30*, 3943 – 3946; b) S. V. Campos, L. P. Miranda, M. Meldal, *J. Chem. Soc. Perkin Trans. 1* **2002**, 682 – 686.
[6] K. Barlos, D. Gatos, S. Kapolos, G. Papaphotiu, W. Schafer, W. Q. Yao, *Tetrahedron Lett.* **1989**, *30*, 3947 – 3950.
[7] K. Kitagawa, C. Aida, H. Fujiwara, T. Yagami, S. Futaki, *Tetrahedron Lett.* **1997**, *38*, 599 – 602.
[8] K. Kitagawa, C. Aida, H. Fujiwara, T. Yagami, S. Futaki, M. Kogire, J. Ida, K. Inoue, *J. Org. Chem.* **2001**, *66*, 1 – 10.
[9] See reference [2b] and T. Young, Ph.D. thesis, University of Wisconsin (Madison), **2001**.
[10] B. Loubinoux, S. Tabbache, P. Gerardin, J. Miazimbakana, *Tetrahedron* **1988**, *44*, 6055 – 6064.
[11] E. F. V. Scriven, K. Turnbull, *Chem. Rev.* **1988**, *88*, 297 – 386.
[12] a) T. Benneche, K. Undheim, *Acta Chem. Scand. B* **1983**, *37*, 93 – 96; b) P. J. Garegg, *Adv. Carbohyd. Chem. Biochem.* **1997**, *52*, 179 – 205.
[13] For a detailed description of various conditions for activation of **3**, see the Supporting Information.
[14] a) M. Sakaitani, Y. Ohfune, *Tetrahedron Lett.* **1985**, *26*, 5543 – 5546; b) A. J. Zhang, D. H. Russell, J. P. Zhu, K. Burgess, *Tetrahedron Lett.* **1998**, *39*, 7439 – 7442.
[15] J. Paladino, C. Guyard, C. Thurieau, J. L. Fauchere, *Helv. Chim. Acta* **1993**, *76*, 2465 – 2472.
[16] a) T. R. Burke, M. S. Smyth, A. Otaka, P. P. Roller, *Tetrahedron Lett.* **1993**, *34*, 4125 – 4128; b) S. F. Liu, C. Dockendorff, S. D. Taylor, *Org. Lett.* **2001**, *3*, 1571 – 1574.
[17] See the Supporting Information for the structure. Crystal data for $C_{26}H_{24}N_4O_5$: Crystal size = $0.09 \times 0.02 \times 0.02$ mm^3, orthorhombic, $P2_12_12_1$, $a = 5.0195(5)$, $b = 19.2028(12)$, $c = 24.566(2)$ Å, $V = 2367.9(3)$ Å^3, $D_{calcl} = 1.325$ mg m^{-3}, $2\theta_{max} = 41.06°$, $Ag_{K\alpha}$ radiation ($\lambda = 0.5594$ Å), ω scans, $T = 173(1)$ K, 26122 independent and 2803 unique reflections. The data were corrected for Lorentz and polarization effects, the empirical absorption correction was performed with SADABS as described in R. H. Blessing, *Acta Crystallogr. Sect. A* **1995**, *51*, 33 – 38, $\mu = 0.058$ mm^{-1}, $T_{max}/T_{min} = 0.9988/0.9948$. The structure was solved and refined with the program package SHELXTL (version 5.1) program library (G. Sheldrick, Bruker Analytical X-Ray Systems, Madison, WI). All non-hydrogen atoms were refined with anisotropic displacement coefficients. All hydrogen atoms were included in the structure-factor calculation at idealized positions. The final least-squares refinement of 317 parameters against 2803 data resulted in residual factors R (based on F^2 for $I \geq 2\sigma$) and wR (based on F^2 for all data) of 0.0667 and 0.2167, respectively. The final difference Fourier map was featureless. CCDC-188441 (**1**) contains the supplementary crystallographic data for this paper. These data can be obtained free of charge via www.ccdc.cam.ac.uk/conts/retrieving.html (or from the Cambridge Crystallographic Data Centre, 12, Union Road, Cambridge CB2 1EZ, UK; fax: (+44) 1223-336-033; or deposit@ccdc.cam.ac.uk).
[18] For details, see the Supporting Information.
[19] M. Bartra, P. Romea, F. Urpi, J. Vilarrasa, *Tetrahedron* **1990**, *46*, 587 – 594.
[20] Y. Matsubayashi, H. Hanai, O. Hara, Y. Sakagami, *Biochem. Biophys. Res. Commun.* **1996**, *225*, 209 – 214.
[21] D. Sako, X. J. Chang, K. M. Barone, G. Vachino, H. M. White, G. Shaw, G. M. Veldman, K. M. Bean, T. J. Ahern, B. Furie, D. A. Cumming, G. R. Larsen, *Cell* **1993**, *75*, 1179 – 1186.
[22] a) D. Sako, K. M. Comess, K. M. Barone, R. T. Camphausen, D. A. Cumming, G. D. Shaw, *Cell* **1995**, *83*, 323 – 331; b) T. Pouyani, B. Seed, *Cell* **1995**, *83*, 333 – 343.
[23] For syntheses of other sulfated peptides derived from PSGL-1, see: a) A. Leppanen, P. Mehta, Y. B. Ouyang, T. Z. Ju, J. Helin, K. L. Moore, I. van Die, W. M. Canfield, R. P. McEver, R. D. Cummings, *J. Biol. Chem.* **1999**, *274*, 24838 – 24848; b) K. M. Koeller, M. E. B. Smith, R. F. Huang, C. H. Wong, *J. Am. Chem. Soc.* **2000**, 122, 4241 – 4242; c) P. Durieux, J. Fernandez-Carneado, G. Tuchscherer, *Tetrahedron Lett.* **2001**, *42*, 2297 – 2299.
[24] See reference [23] and C. R. Bertozzi, L. L. Kiessling, *Science* **2001**, *291*, 2357 – 2364.

Nanotubes of Group 4 Metal Disulfides**

Manashi Nath and C. N. R. Rao*

Since the discovery of the carbon nanotubes, there has been active interest in exploring whether other layered materials, especially metal disulfides such as MoS_2 and WS_2, form nanotubes and related structures. Tenne et al.[1,2] succeeded in preparing nanotubes of MoS_2 and WS_2 by first heating the metal oxide in a stream of forming gas (95 % N_2 + 5 % H_2) followed by reaction with H_2S at elevated temperatures (700–1000 °C). Thermal decomposition of the ammonium thiometallate $(NH_4)_2MS_4$ (M = Mo or W) in a H_2 atmosphere has been employed recently to obtain the disulfide nanotubes.[3] Metal trisulfides are formed as intermediates in the formation of the disulfide nanotubes in both of the above methods. Accordingly, MoS_2 and WS_2 nanotubes could be prepared directly from the decomposition of MoS_3 and WS_3 in a hydrogen atmosphere.[3] NbS_2 nanotubes have also been prepared by the thermal decomposition of NbS_3 in a hydrogen atmosphere at 1000 °C.[4] These results suggested that it may indeed be possible to prepare nanotubes of other layered disulfides by the thermal decomposition of appropriate trisulfide precursors. Since the disulfides of Group 4 metals, such as Ti, Zr, and Hf, possess layered hexagonal structures,[5,6] we considered it feasible to prepare the nanotubes of these materials starting from their trisulfides. Herein we

[*] Prof. Dr. C. N. R. Rao, M. Nath
CSIR Centre For Excellence In Chemistry and
Chemistry and Physics of Materials Unit
Jawaharlal Nehru Centre for Advanced Scientific Research
Jakkur P.O., Bangalore 560 064 (India)
E-mail: cnrrao@jncasr.ac.in
and
Solid State And Structural Chemistry Unit
Indian Institute of Science
Bangalore 560 012 (India)
Fax: (+91) 80-846-2760

[**] The authors thank the DRDO (India) for research support and Mr. Md. Motin Seikh and Dr. N. Chandrabhas for help with the Raman measurements.

  0044-8249/02/4118-3451 $ 20.00+.50/0

report the first successful synthesis and characterization of these nanotubes of the Group 4 metal disulfides.

Thermal decomposition of HfS_3 at 900 °C in an atmosphere of Ar(95 %) + H_2(5 %) gave a good yield of nanostructures as evident from the scanning electron microscope (SEM) image (Figure 1 a). Analysis by energy-dispersive X-ray spectroscopy (EDX) showed the Hf:S ratio to be 1:2. The

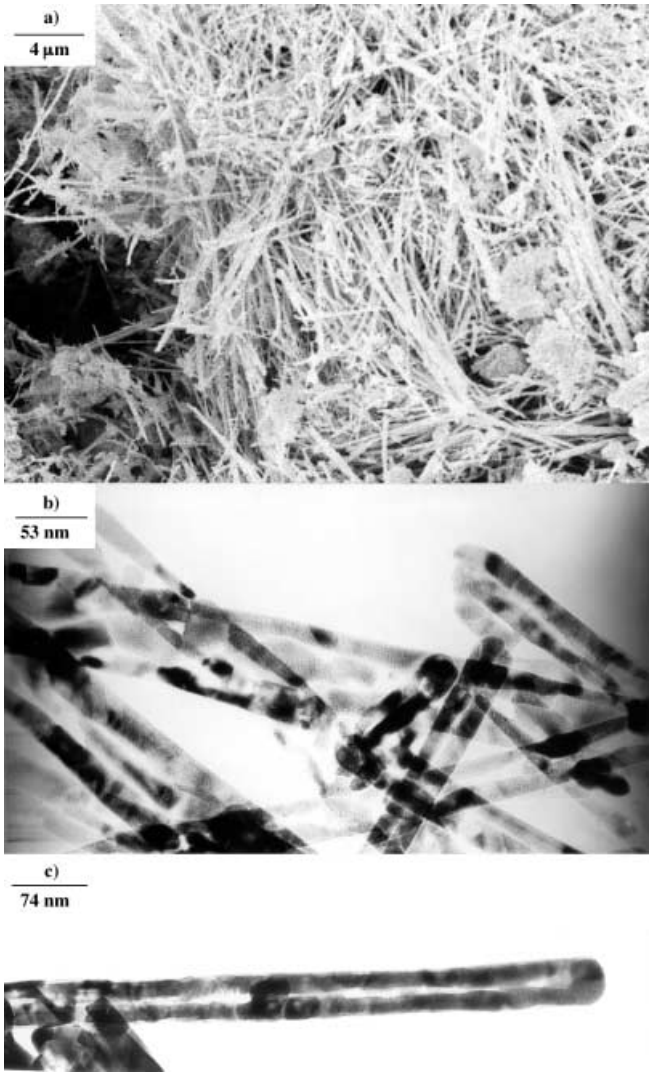

Figure 1. a) SEM image showing a large collection of HfS_2 nanostructures, some being more than a micron long; b) and c) low-resolution TEM images of the HfS_2 nanotubes with closed caps.

powder X-ray diffraction (XRD) pattern of the product confirmed it to be 1T-HfS_2, with the lattice parameters $a =$ 3.635 and $c = 5.851$ Å (JCPDS card No. 28-0444). There is a slight expansion (ca. 1 %) in the *c*-axis of the nanostructures. The expansion is much smaller than that observed in the MoS_2 and WS_2 nanotubes (ca. 3 %),[1b] possibly because the mean *c*-axis compressibility of HfS_2 is higher than that of MoS_2.[7] The nanostructures are typically more than a micron long, with a large proportion of them being nanotubes. A low magnification transmission electron microscope (TEM) image of the nanotubes is shown in Figure 1 b. A TEM image of a nanotube with a length greater than 500 nm is shown in Figure 1 c. The outer diameter of the nanotubes is in the range of 55–60 nm, while the inner core diameter is around 17–30 nm. The diameter of some of the nanotubes varies along the length. Thus, the nanotube in Figure 1 c has an outer diameter of 40 nm and an inner diameter in the range of 7–13 nm. These nanotubes have non-uniform walls and generally have non-spherical tips, with some being rectangular.

The TEM image of a HfS_2 nanotube with a rectangular tip is shown in Figure 2 a. At the outer corners of the tip there are ripplelike undulations which can arise from the strain

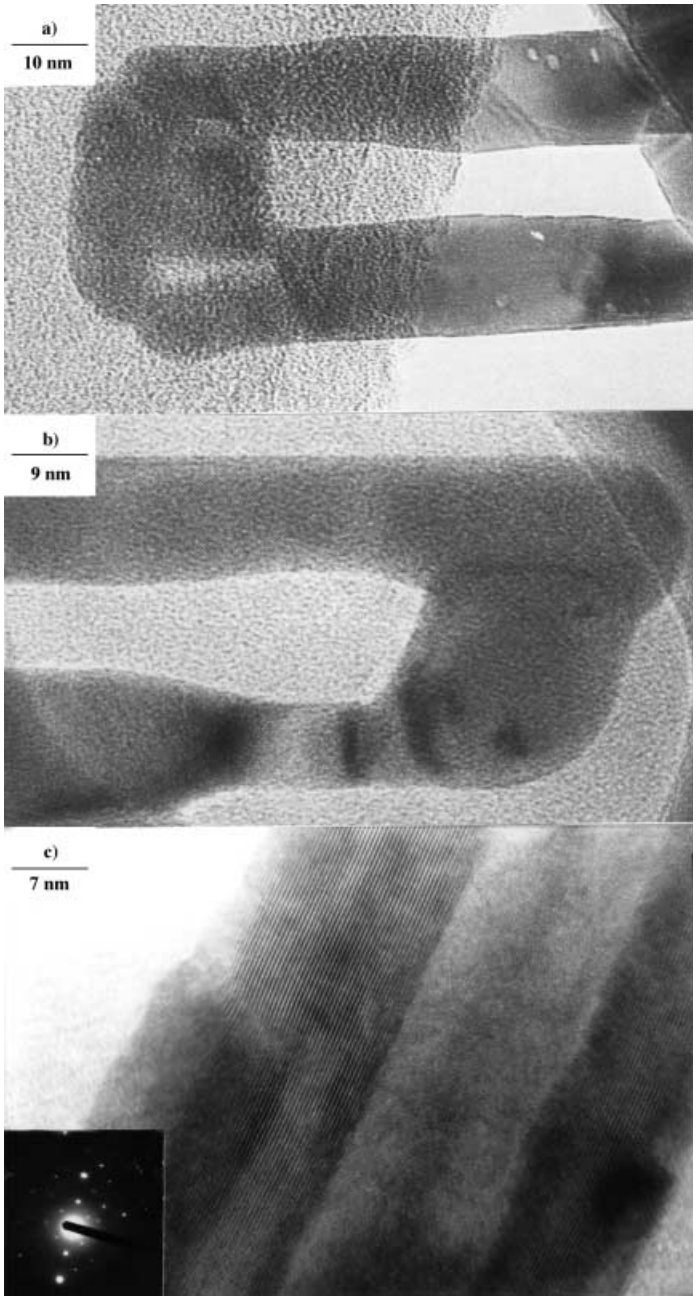

Figure 2. a) Low-resolution TEM image of HfS_2 nanotubes; b) TEM image of a HfS_2 nanotube with layer fringes at an angle to the tube axis; c) high-resolution TEM image of a HfS_2 nanotube showing layer fringes with a separation of 5.8 Å. The tube axis is perpendicular to the *c* direction. The inset in (c) shows the ED pattern exhibiting a hexagonal arrangement of layers.

  0044-8249/02/4118-3452 $ 20.00+.50/0

involved in bending the layers. Layer fringes are visible along the tube walls on close inspection. Terminated layers occur both in the outer and inner edges of the wall, which causes non-uniformity in the wall thickness. Such rectangular tips have been observed in the nanotubes of MoS_2, WS_2, and $Mo_{1-x}W_xS_2$ nanotubes.[8,9] The image of the nanotube in Figure 2b shows an unusual rectangular tip, and the layer fringes along the tube walls show a layer separation of approximately 5.8 Å (the separation between (001) planes in bulk HfS_2 is 5.84 Å). The layers are, however, not parallel to the tube axis as expected, and instead make an angle of about 40° with the tube axis; in other words, the tube axis is at an angle of 40° to the *c* direction.

Figure 2c shows a high-resolution image of a HfS_2 nanotube with the tube axis perpendicular to the *c*-direction. The layer separation here is approximately 5.8 Å. We observe several terminated layers at the outer edges of the tube walls, possibly as a result of the absence of growing material at the edges. A considerable number of defects and edge dislocations seem to be present along the length of the tube wall. The inset in Figure 2c shows an electron diffraction (ED) pattern characteristic of the hexagonal arrangement of the *d*(101) layers. The ED pattern also contains Bragg spots corresponding to the *d*(002) plane (2.923 Å). Overall, the ED pattern indicates the tube axis to be perpendicular to the *c*-direction.

The growth of the HfS_2 nanotubes appears to start from the HfS_3 particles. The first disulfide layers formed initially entrap the trisulfide particles and inhibit the formation of larger aggregates. HfS_3 then decomposes to form the HfS_2 layers, which grow outward from the precursor particle to form tubules. As a consequence of such growths, defects and edge dislocations occur near the tube tip and walls, which are the active points for tube growth.

We have recorded the electronic absorption and emission spectra of the HfS_2 nanotubes. HfS_2 is an indirect band-gap semiconductor with an indirect band gap energy of about 2 eV.[10] The reflectance spectrum of bulk HfS_2 shows a band with a maximum at 550 nm and a sharper band at 250 nm. The nanotubes show a small blue-shift of the longer wavelength band. The photoluminescence spectrum of the nanotubes shows a peak at 676 nm, while the bulk sample has a band at 687 nm (Figure 3a). This feature is likely to arise from sub-band-gap emission or from gap states.

The Raman spectrum of the HfS_2 nanotubes has a band arising from the A_{1g} mode, which corresponds to the S atom vibration along the *c*-axis perpendicular to the basal plane, and another arising from the E_g mode as a consequence of the movement of the S and Hf atoms in the basal plane.[11] The Raman bands of the nanotube correspond exactly to the bands obtained for the bulk HfS_2 powder, but the A_{1g} band shows some broadening. The full-width at half maximum (FWHM) of the A_{1g} band is 11 cm^{-1} in the nanotubes compared to 8 cm^{-1} for the bulk sample. Such a broadening of the Raman band has been noted in MoS_2 and WS_2 nanotubes.[12] The broadening of the Raman band in the nanotubes can be explained by the spatial correlation or the phonon confinement model, which predicts a broadening of the Raman signal as the crystallite decreases.[13] The decrease in the crystallite size relaxes the $\Delta q = 0$ selection rule, thus

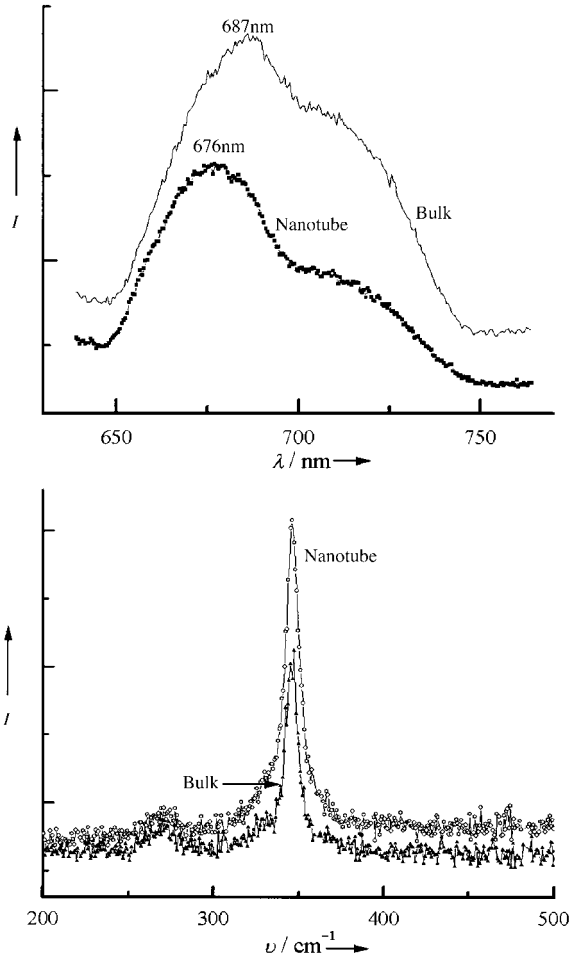

Figure 3. a) Photoluminescence spectra of nanotubes and a bulk sample of HfS_2; b) Raman spectra of the nanotubes and a bulk sample of HfS_2.

allowing transitions with $q \neq 0$, which in effect cause a broadening of the signal.

We have been able to obtain nanotubes of ZrS_2 by the thermal decomposition of ZrS_3, under conditions similar to those mentioned earlier for HfS_2. The powder XRD pattern of the decomposed product showed it to possess the hexagonal structure with $a = 3.660$ and $c = 5.825$ Å (JCPDS card No. 11-0679). EDX analysis confirmed the composition. The low-resolution TEM image (Figure 4a) shows a ZrS_2 nanotube with a closed rectangular tip. The outer diameter of the tube is approximately 125 nm, while the inner core diameter is about 60 nm. Besides nanotubes, nanorods and onions are also seen in the images. The nanotube in Figure 4b, also with a rectangular tip, contains undulations at the outer edge, just as in HfS_2 nanotubes, with the inner wall showing non-uniformity resulting from the discontinuous growth of the ZrS_2 layers. Figure 4c shows nanotubes with diameters of about 140 nm and possessing fairly linear uniform walls. The inset of Figure 4c shows an ED pattern with the characteristic hexagonal arrangement of the (101) layers and containing Bragg spots corresponding to *d*(002).

We were able to prepare TiS_2 nanotubes by the thermal decomposition of TiS_3 in a H_2 + He atmosphere at 800 °C. These nanotubes were more beam sensitive, but we could, however, obtain low-resolution TEM images.

  0044-8249/02/4118-3453 $ 20.00+.50/0

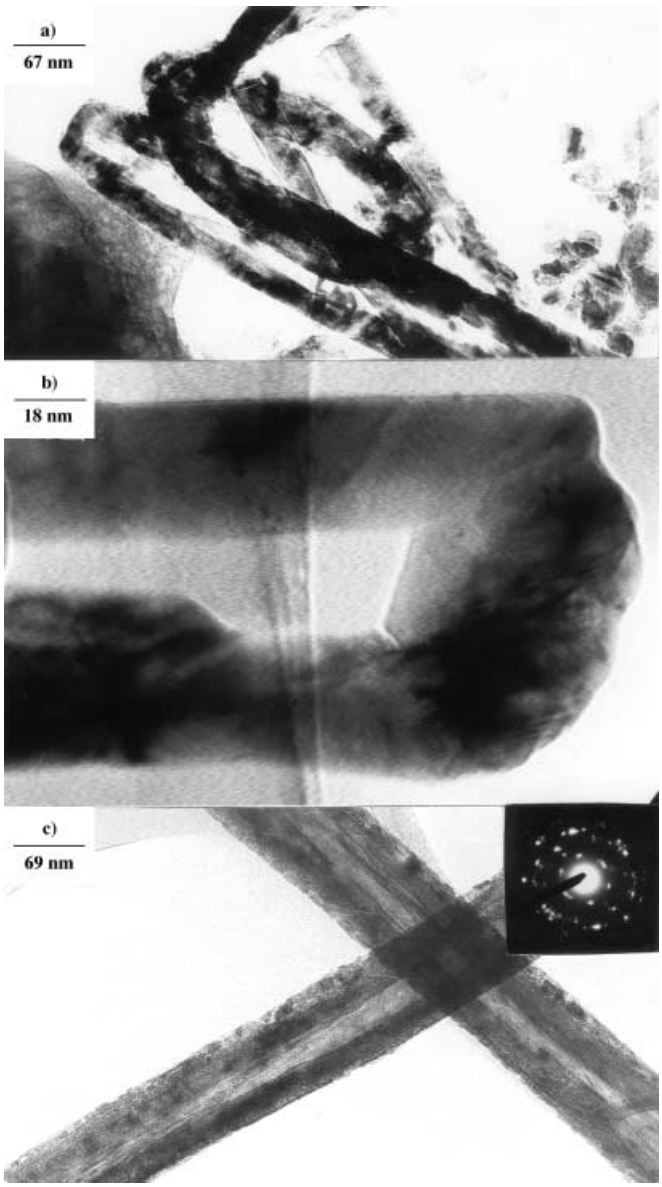

Figure 4. Low-resolution TEM images of the ZrS_2 nanotubes. The tubes in images (b) and (c) show rectangular tips. The inset in (c) shows a typical ED pattern.

In conclusion, nanotubes of the disulfides of the three Group 4 metals, Hf, Zr, and Ti have been successfully prepared by the decomposition of the corresponding trisulfides in a reducing atmosphere.

Experimental Section

The trisulfides were synthesized in a sealed-tube reaction by the direct combination of the elements.[5,6] In a typical synthesis Hf and S powders were mixed in a stoichiometric ratio and the mixture sealed in a quartz ampoule under vacuum. The ampoule was placed in a furnace, which was raised slowly to 560 °C and maintained at that temperature for 36 h. HfS_3 formed as a bright orange solid.

The trisulfides were decomposed in a stream of Ar and H_2 around 900 °C to obtain the disulfide nanotubes. The HfS_3 powder was placed in the central zone of a horizontal furnace, the temperature of which was slowly raised to 900 °C (heating rate of 10 °C min^{-1}), and a steady flow of a mixture of Ar (285 standard cubic centimeters (sccm)) and H_2 (15 sccm) was maintained. The decomposition was carried out for 40 min, after which the temperature of the furnace was reduced. A dark brown powder containing HfS_2 nanostructures were obtained.

Powder X-ray diffraction patterns were obtained using a Seifert diffractometer. SEM images and EDX analysis was carried out using a Leica S440I instrument equipped with ISIS Link software. TEM images were obtained by using a JEOL JEM-3010 transmission electron microscope operating at 300 kV. The HfS_2 and ZrS_2 nanotubes were quite beam-stable, unlike the TiS_2 nanotubes. Photoluminescence studies were performed with a Perkin Elmer LS 55 luminescence spectrometer. Raman measurements were performed with a solid-state Nd-YAG laser and an excitation of 532 nm.

Received: April 12, 2002
Revised: June 28, 0000 [Z19080]

[1] a) R. Tenne, L. Margulis, M. Genut, G. Hodes, *Nature* **1992**, *360*, 444; b) Y. Feldman, E. Wasserman, D. J. Srolovitch, R. Tenne, *Science* **1995**, *267*, 222; c) L. Margulis, G. Salitra, M. Taliankar, R. Tenne, *Nature* **1993** *365*, 113.
[2] R. Tenne, M. Homyonfer, Y. Feldman, *Chem. Mater.* **1998**, *10*, 3225.
[3] M. Nath, A. Govindaraj, C. N. R. Rao, *Adv. Mater.* **2001**, *13*, 283.
[4] M. Nath, C. N. R. Rao, *J. Am. Chem. Soc.* **2001**, *123*, 4841.
[5] Mc. Taggart, A. D. Wadsley, *Aust. J. Chem.* **1958**, *11*, 445.
[6] C. N. R. Rao, K. P. R. Pisharody, *Prog. Solid State Chem.* **1975**, *10*, 207.
[7] H. D. Falck, *J. Appl. Crystallogr.* **1972**, *5*, 138.
[8] Y. Q. Zhu, W. K. Hsu, H. Terrones, N. Grobert, B. H. Chang, M. Terrones, B. Q. Wei, H. W. Kroto, D. R. M. Walton, C. B. Boothroyd, I. Kinloch, G. Z. Chen, A. H. Windle, D. J. Fray, *J. Mater. Chem.* **2000**. *10*, 2570.
[9] M. Nath, K. Mukhopadhyay, C. N. R. Rao, *Chem. Phys. Lett.* **2002**, *352*, 163.
[10] a) L. E. Conroy, K. C. Park, *Inorg. Chem.* **1968**, *7*, 459; b) D. L. Greenaway, R. Nitsche, *J. Phys. Chem. Solids* **1965**, *26*, 1445.
[11] a) M. I. Nathan, M. W. Shafer, J. E. Smith, *Bull. Am. Phys. Soc.* **1972**, *17*, 336; b) L. Roubi, C. Carlone, *Phys. Rev. B* **1988**, *37* 6808.
[12] G. L. Frey, R. Tenne M. J. Matthews, M. S. Dresselhaus, G. Dresselhaus, *J. Mater. Res.* **1998**, *13*, 2412.
[13] a) H. Richter, Z. P. Wang, L. Ley, *Solid State Commun.* **1981**, *39*, 625; b) T. Kanata, H. Murai, K, Kubota, *J. Appl. Phys.* **1987**, *61*, 969.

A Straightforward NMR-Spectroscopy-Based Method for Rapid Library Screening**

Aloysius H. Siriwardena,* Fang Tian, Schroder Noble, and James H. Prestegard

A variety of NMR-based methods have been devised to facilitate the screening of compound mixtures for components that bind protein drug targets.[1–6] The majority of these approaches have been developed in recent years, hand in hand with methods for generating libraries of compounds by combinatorial chemistry.[7] The ability to screen such libraries rapidly and simply to identify potential leads is an important

[*] Prof. Dr. A. H. Siriwardena, Dr. F. Tian, S. Noble, Prof. Dr. J. H. Prestegard
The Complex Carbohydrate Research Center
University of Georgia
220, Riverbend Road, Athens, GA 30602—4712 (USA)
Fax: (+1) 706-542-4412
E-mail: siriward@ccrc.uga.edu

[**] AHS wishes to thank Dr H. Al-Hashimi (Ann Arbor) and Dr Nitin U. Jain (UGA) for fruitful discussions. This work was supported by the NIH (Grant: RR05351).

  0044-8249/02/4118-3454 $ 20.00+.50/0